Non-Equilibrium Thermal Degradation and Iso-conversional Kinetics of Norway Spruce (Picea abies) under Inert and Oxidative Atmospheres

Andrea Majlingova

majlingova@tuzvo.sk

Technical University in Zvolen

Viktoria – Barna

Technical University in Zvolen

Qiang Xu

Nanjing University of Science and Technology

Research Article

Keywords: Activation energy, char formation, iso-conversional kinetics, non-equilibrium pyrolysis, Norway spruce (Picea abies), simultaneous thermal analysis, oxidative degradation.

Posted Date: June 17th, 2026

DOI: https://doi.org/10.21203/rs.3.rs-9907692/v1

Additional Declarations: No competing interests reported.

Non-Equilibrium Thermal Degradation and Iso-conversional Kinetics of Norway Spruce (*Picea abies*) under Inert and Oxidative Atmospheres

Majlingova, Andrea[1,*] – Barna, Viktoria[1] – Xu Qiang[2]

1 Department of Fire Protection, Faculty of Wood Sciences and Technology, Technical University in Zvolen, T. G. Masaryka 24, 960 01 Zvolen, Slovakia

2 School of Mechanical Engineering, Nanjing University of Science and Technology, Xiao Ling Wei 200, Nanjing, Jiangsu Province, P. R. China

Corresponding author:
Andrea Majlingova
E-mail: majlingova@tuzvo.sk

ORCID:
Andrea Majlingova: 0000-0002-7450-4004
Viktória Barna: 0009-0003-8535-5950
Qiang Xu: 0009-0002-9751-3955

Acknowledgments

The authors acknowledge the financial support from the Slovak Research and Development Agency, Grant No. APVV-22-0030 and Grant number APVV-SK-CN-23-0001.

ABSTRACT

The non-isothermal thermal degradation of Norway spruce wood (Picea abies (L.) H. Karst.) was investigated by simultaneous thermogravimetry and differential scanning calorimetry under nitrogen and synthetic air atmospheres at heating rates of 10, 25 and 50 °C min^{-1}. The aim was to evaluate the effects of atmosphere and heating rate on degradation behavior and apparent kinetic parameters using model-free methods. Under nitrogen, the process proceeded through four degradation regions: moisture release, hemicellulose decomposition, a dominant cellulose-related mass-loss stage and high-temperature char consolidation. The temperature of the main DTG peak increased from 619.5 to 638.0 K with increasing heating rate, while the residual mass at 500 °C increased from 21.5 to 27.1%, indicating enhanced char retention under non-equilibrium heating conditions. In synthetic air, two main mass-loss stages were observed, corresponding to oxidative pyrolysis and subsequent char combustion. The main degradation peak occurred at lower temperatures than under nitrogen, whereas the second stage was accompanied by a pronounced exothermic DSC effect above 700 K. Residual mass under air was below 5% at 10 and 25 °C min^{-1}, confirming near-complete oxidation of the char residue. The Kissinger method yielded apparent activation energies of 262.1 kJ mol-1 under nitrogen and 190.1 kJ mol-1 under synthetic air. Iso-conversional analysis by the Ozawa–Flynn–Wall and Kissinger–Akahira–Sunose methods showed a nearly constant activation energy profile under nitrogen, with mean values of 341 and 348 kJ mol-1, respectively. Lower and more variable values were obtained under synthetic air because of overlapping pyrolytic and oxidative reactions. The results provide a consistent thermal and kinetic characterization of spruce wood degradation under inert and oxidative conditions and demonstrate the importance of atmosphere and heating rate in the interpretation of wood thermal decomposition.

Keywords

Activation energy; char formation; iso-conversional kinetics; non-equilibrium pyrolysis; Norway spruce (*Picea abies*); simultaneous thermal analysis; oxidative degradation.

Statements and Declarations

Competing Interests

The authors declare that they have no competing financial or non-financial interests related to this work.

Funding

This work was supported by the Slovak Research and Development Agency under the contract No. APVV-22-0030 and contract No. APVV-SK-CN-23-0001.

Author Contributions

Conceptualization: Andrea Majlingova, Qiang Xu; Methodology: Andrea Majlingova;
Investigation: Viktoria Barna; Data analysis: Andrea Majlingova, Qiang Xu; Writing – original draft: Viktoria Barna, Andrea Majlingova; Writing – review and editing: All authors.

All authors read and approved the final manuscript.

Data Availability

The datasets generated and analyzed during the current study are available from the corresponding author on reasonable request.

1. Introduction

The thermal degradation of lignocellulosic biomass has attracted sustained scientific interest, driven by the dual imperatives of transitioning toward renewable energy sources and understanding the fire behavior of solid biomass materials [1, 2]. Wood represents a canonical substrate for fundamental studies of thermal decomposition, pyrolysis, and oxidative combustion owing to its chemical well-characterization and global abundance [3]. Among European conifers, Norway spruce (*Picea abies* (L.) H. Karst.) occupies a particularly important position: it is the dominant commercial timber species across Central and Northern Europe and one of the most widely studied softwoods in thermochemical conversion research [4]. Its relatively low moisture retention after drying and high resin content make it a relevant substrate for both bioenergy applications and fire science.

The thermal degradation of wood proceeds through a sequence of overlapping reactions governed by the distinct decomposition kinetics of its three principal structural components: hemicellulose, cellulose, and lignin [5, 6]. As demonstrated by Yang et al. [5], hemicellulose undergoes rapid mass loss in the range 220–315 °C, cellulose decomposes predominantly between 315 and 400 °C, while lignin degrades over a broad temperature interval extending from approximately 160 to 900 °C, producing substantially higher char yields. Grønli et al. [7] further showed that softwoods, including spruce, exhibit earlier onset of decomposition, a more delayed hemicellulose shoulder, and wider hemicellulose and cellulose degradation zones compared with hardwoods, differences attributable to the distinct hemicellulose composition (galactoglucomannans vs. xylans) and the higher extractive content of conifers. The interplay of these parallel and sequential reactions gives rise to a multi-step kinetic character that single-step models are unable to capture adequately [8, 9, 10].

Simultaneous thermal analysis (STA), combining thermogravimetry (TG) with differential scanning calorimetry (DSC) in a single measurement, provides a comprehensive and internally consistent experimental basis for kinetic characterization of solid-state thermal decomposition [11]. The concurrent acquisition of mass-change and heat-flow signals under identical atmospheric and thermal conditions eliminates the ambiguities that arise when TG and DSC data are collected separately. The derivative TG (DTG) curve enables precise identification of characteristic temperatures and stage intensities, while the DSC signal distinguishes endothermic depolymerization from exothermic char oxidation events [5].

Model-free iso-conversional kinetic methods, in which the activation energy E_a is determined as a function of conversion α without prior assumption of a reaction model, have become the recommended approach for thermally complex, multi-step systems [8–10]. The Ozawa–Flynn–Wall (OFW) method [12, 13] and the Kissinger–Akahira–Sunose (KAS) integral method [14] exploit the dependence of the temperature at a given conversion on the applied heating rate β. By performing measurements at multiple heating rates, the variation of $E_a(\alpha)$) across the full conversion range can be mapped, revealing kinetic transitions corresponding to changes in the rate-limiting

reaction mechanism. The complementary Kissinger peak method [15] yields a single apparent activation energy from the shift of the DTG maximum with heating rate and is widely used as a benchmark for literature comparison.

The heating rate exerts a well-documented influence on the thermal degradation behavior of biomass [7, 16]. Under slow heating conditions the system approaches quasi-equilibrium and individual decomposition stages are better resolved. At elevated heating rates, thermal lag shifts characteristic temperatures to higher values and modifies the competitive balance between parallel reaction channels, leading to altered product distributions and char yields [17]. Heating rates of 50 °C min-1 and above, while less common in conventional thermokinetic studies, approach conditions relevant to fire scenarios and flash pyrolysis reactors, where the assumption of thermodynamic equilibrium is no longer tenable [18]. Characterizing this non-equilibrium regime thus requires explicit treatment of heating-rate effects.

The classification of thermal conversion conditions as low or high heating rate is not merely a methodological distinction but carries direct physical significance. Mehrabian et al. [19] showed, using a validated single-particle pyrolysis model, that 50 K min-1 represents the practical upper boundary of the low heating rate regime: above this threshold, kinetic parameters derived from conventional TGA measurements are no longer applicable to industrially relevant biomass conversion systems such as pulverized wood combustion and pellet gasification, in which particles invariably operate in the high heating rate regime. The maximum heating rate of 50 °C min-1 employed in the present study therefore represents a boundary condition between the quasi-equilibrium and non-equilibrium kinetic regimes, i.e. a thermodynamically extreme condition relative to standard analytical practice [8–10, 19]. At this boundary, the competition between primary devolatilization and secondary char-forming repolymerization reactions is no longer resolved at the time scale of the thermal ramp, leading to measurable deviations in char yield and product distribution from equilibrium predictions [3]. In the context of structural fire scenarios, the surface of a wood element exposed to a growing fire can experience local heating rates ranging from approximately 5 to over 50 °C min-1 depending on incident heat flux and wood geometry [20], placing the upper bound of the present experimental range directly within fire-relevant conditions. Characterizing the kinetic response of spruce wood across this full range therefore provides data applicable to both thermochemical conversion engineering and fire safety assessment.

The surrounding atmosphere profoundly modifies the degradation pathway. Under nitrogen, the process is purely pyrolytic: primary decomposition products either volatilize or undergo secondary char-forming reactions with no oxidative contribution. In synthetic air, an additional exothermic char combustion stage superimposes on the pyrolytic mass-loss events, substantially altering the DTG and DSC profiles and lowering residual mass [16, 17]. Separate kinetic analysis under inert and oxidative atmospheres is therefore essential for disentangling pyrolysis kinetics from oxidation kinetics and for generating input parameters relevant to fire modeling.

Although thermal analysis does not directly identify the molecular composition of volatile degradation products, the assignment of the main TG/DTG/DSC stages can be interpreted in relation to established degradation pathways of lignocellulosic components [21, 22]. Previous studies on biomass pyrolysis, e.g. [23, 24], have shown that cellulose degradation is commonly associated with anhydro sugar formation, whereas hemicellulose and lignin decomposition may contribute to furanic, carbonyl and phenolic products. In the present study, however, the focus is restricted to the thermal and kinetic response of Norway spruce evaluated by TG/DTG/DSC; direct molecular identification of volatile products is outside the scope of this paper.

The present study investigates the non-isothermal thermal degradation of Norway spruce wood at heating rates of 10, 25 and 50 °C min^{-1} under nitrogen and synthetic air atmospheres using a NETZSCH STA 509 Jupiter® Classic instrument. Characteristic temperatures, mass-loss parameters and residual mass are reported for all experimental conditions. Conversion-dependent activation energies are determined by the Ozawa–Flynn–Wall and Kissinger–Akahira–Sunose iso-conversional methods and benchmarked against the Kissinger peak method. The results are interpreted in terms of the multi-component degradation mechanism of spruce wood and the influence of heating rate and atmosphere on non-equilibrium thermal behavior.

2. Methodology

2.1 Material Preparation

Spruce wood (*Picea abies (L.)* H. Karst.) without bark was obtained from a University Forest Enterprise, Technical University in Zvolen. The material was mechanically milled using a cutting mill (PULVERISETTE 15, FRITSCH GmbH – Milling and Sizing, Idar-Oberstein, Germany) and sieved (AS 200 basic, RETSCH GmbH, Haan, Germany) to obtain a particle-size fraction of 100–250 µm. Prior to analysis, the sample was dried at 105 °C for 24 h to constant mass in a drying oven and subsequently cooled in a desiccator. The dried material was stored in a sealed desiccator until measurement to prevent moisture uptake.

2.2 Simultaneous Thermal Analysis

Thermal degradation was investigated by simultaneous thermogravimetry and heat-flow calorimetry (TG/DSC) using a NETZSCH STA 509 Jupiter(R) Classic instrument (NETZSCH-Geraetebau GmbH, Selb, Germany). Approximately 5–9 mg of sample was placed in an open Al_2O_3 crucible (85 µL) and distributed as a thin, uniform layer to minimize thermal gradients and promote uniform gas-solid contact. The reference position was left empty throughout all experiments.

Measurements were performed in the temperature range 25–500 °C under non-isothermal dynamic conditions without isothermal holding segments. Three nominal heating rates (β) were applied: 10, 25 and 50 °C min^{-1}. Two atmospheres were used in separate experimental series: inert nitrogen (N_2, purity 99.999%, Grade 6.0) and synthetic air (approximately 21% O_2, balance N_2), both supplied at a constant flow rate of 60 mL min^{-1}. A protective nitrogen purge flow of 50 mL min^{-1} was maintained throughout all runs. Each combination of heating rate and atmosphere was measured in triplicate (n = 3), yielding 18 independent experimental runs in total.

From the TG and DTG curves, the following characteristic temperatures were determined for each run: onset temperature (T_{onset}), temperature of maximum mass-loss rate (T_{max}, i.e., the minimum of the DTG curve), and endset temperature (T_{end}). T_{onset} and T_{end} were defined as the points at which the rate of mass change exceeded and fell below 5% of the absolute DTG peak value, respectively, after the initial moisture-loss region (T > 150 °C). Residual mass at the end of the temperature program and total mass loss across the main degradation stage were also recorded. All mass values are reported as percentages of the initial sample mass.

2.3 Kinetic Evaluation

The degree of conversion α was calculated from the TG data according to:

$$\alpha = \frac{m_0 - m(T)}{m_0 - m_f}$$

where m_0 is the initial mass at the beginning of the selected degradation interval, $m(T)$ is the mass at temperature T, and m_f is the final mass at the end of the selected interval. The conversion range α = 0.05–0.90 was used for iso-conversional analysis; values outside this range were excluded to avoid artefacts associated with noise at the beginning and end of the decomposition event.

Activation energy as a function of conversion, $E_a(\alpha)$, was determined by two model-free iso-conversional methods.

Ozawa-Flynn-Wall (OFW) method. The OFW method is based on the integral iso-conversional approximation [1, 2]. At a fixed conversion level, the following linearization applies:

$$log\beta = -0.4567\left(\frac{E_a}{R}\right)\left(\frac{1}{T_\alpha}\right) + const$$

where β is the heating rate (°C min-1), Tα is the absolute temperature (K) at which conversion α is reached, E_a is the activation energy (J mol-1), and R is the universal gas constant (8.314 J mol-1 K-1). For each α, $log\beta$ was plotted against $\frac{1}{T_\alpha}$ and E_a was obtained from the slope via linear regression.

Kissinger–Akahira–Sunose (KAS) method. The KAS method uses the integral iso-conversional approximation of Coats-Redfern and yields improved accuracy relative to OFW [3]. The linearized form is:

$$ln\left(\frac{\beta}{T_{a^2}}\right) = -\frac{E_a}{R\,T_\alpha} + const$$

For each conversion level, $ln\left(\frac{\beta}{T_{a^2}}\right)$ was plotted against $\left(\frac{1}{T_\alpha}\right)$ and E_a was obtained from the linear slope. Both OFW and KAS were applied independently for the N_2 and synthetic air data sets. For each method and conversion level, three heating rates (10, 25, and 50 °C min-1) were used; T_α values were averaged across the three replicates at each heating rate before regression.

Kissinger method. The apparent activation energy corresponding to the maximum mass-loss rate was additionally estimated using the Kissinger peak method [4]:

$$\ln\left(\frac{\beta}{T_{max^2}}\right) = -\frac{E_a}{R\,T_{max}} + const$$

where T_{max} is the absolute temperature (K) of the DTG minimum. The slope of $\ln\left(\frac{\beta}{T_{max^2}}\right)$ plotted against $\frac{1}{T_{max}}$ yields $-\frac{E_a}{R}$. Unlike the iso-conversional methods, the Kissinger method returns a single, conversion-independent apparent activation energy and does not resolve multi-step reaction mechanisms. The goodness of fit of each linear regression was assessed by the coefficient of determination (R^2).

3 Results

3.1 TG and DTG curves – nitrogen atmosphere

3.1.1 General degradation profile and decomposition stages

Under inert nitrogen (N_2), the TG curves of spruce wood recorded at heating rates of 10, 25, and 50 °C min-1 exhibited the characteristic sigmoidal shape associated with lignocellulosic biomass pyrolysis, with the steepest mass loss concentrated between approximately 535 and 700 K (Figure 1a). Excellent reproducibility was observed across the three replicates at each heating rate. Four thermally distinct regions were identified in the combined TG and DTG profiles (Figure 1b).

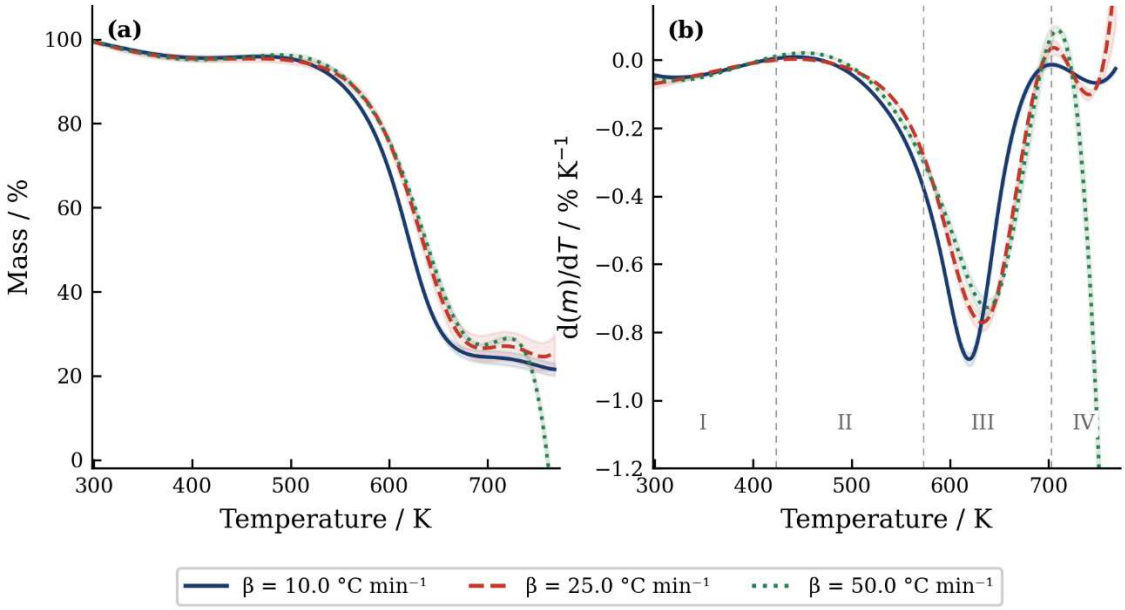

Figure 1. (a) TG curves and (b) DTG curves of Norway spruce wood recorded in nitrogen atmosphere at heating rates of 10, 25, and 50 °C min-1. Solid lines represent mean values of three replicates; shaded bands indicate ±1 standard deviation. Vertical dashed lines in (b) indicate boundaries between thermal decomposition stages I–IV (see text). Stage labels are shown at top of panel (b).

Stage I – Moisture release (298–423 K). A minor mass loss of 1–2% was observed below 423 K, attributed to desorption of physically bound water from the dried sample matrix. This event produced a shallow baseline deflection in the DTG curve and a slightly endothermic contribution to the DSC signal. It was not included in the kinetic analysis.

Stage II – Hemicellulose decomposition (423–573 K). A low-intensity DTG shoulder, most clearly resolved at β = 10 °C min-1, appeared between approximately 493 and 573 K. This feature is characteristic of the deacetylation and depolymerization of O-acetyl-galactoglucomannan (GGM) and arabinoxylan, the dominant hemicellulose types in Norway spruce [5]. The mass loss in this stage was comparatively small, consistent with the lower hemicellulose content of softwoods relative to hardwoods [7]. At higher heating rates (25 and 50 °C min-1), Stage II merged progressively with Stage III, reducing its resolution in the DTG profile.

Stage III – Cellulose depolymerization: main pyrolysis event (543–703 K). The dominant mass-loss event was recorded as a sharp, symmetric DTG minimum centered at T_{max} = 619.5 ± 0.5 K (346.3 ± 0.5 °C) for β = 10 °C min-1, 632.7 ± 0.5 K (359.5 °C) for β = 25 °C min-1, and 638.0 ± 1.3 K (364.9 °C) for β = 50 °C min-1 (Table 1). The corresponding mass loss was 67.3 ± 2.1%, 64.5 ± 2.7%, and 65.5 ± 0.4% at β = 10, 25, and 50 °C min-1, respectively. The event is primarily attributed to glycosidic bond cleavage and depolymerization of cellulose chains. Literature on cellulose pyrolysis commonly associates this stage with the formation of levoglucosan and related anhydro sugar products, although such products were not directly identified in the present study [25].

Table 1 Characteristic temperatures, peak DTG intensity, and mass loss parameters for Norway spruce wood (Picea abies) determined from TG and DTG curves under N_2 and synthetic air atmospheres at three heating rates. Values are means ± 1 standard deviation (n = 3, except β = 50 °C min-1 in air where n = 2).

Parameter	N_2 atmosphere			Synthetic air atmosphere		
	β = 10 / °C min-1	β = 25 / °C min-1	β = 50 / °C min-1	β = 10 / °C min-1	β = 25 / °C min-1	β = 50 / °C min-1
Onset temperature T_{onset} / °C	263.3 ± 1.2	278.2 ± 0.9	270.8 ± 1.3	255.8 ± 2.6	263.5 ± 0.8	268.0 ± 1.6
DTG peak temperature (pyrolysis stage) T_{max} / °C	346.3 ± 0.5	359.5 ± 0.5	364.9 ± 1.3	320.9 ± 0.6[b]	340.1 ± 1.0[b]	339.4 ± 8.3[b]
DTG peak temperature (char combustion, air only) $T_{max,char}$ / °C	-	-	-	447.3 ± 2.7	459.6 ± 16.6*	418.9 ± 55.0*
Endset temperature (pyrolysis stage) T_{end} / °C	413.0 ± 3.3	417.6 ± 2.0	418.9 ± 4.6	-	-	-
Max. mass-loss rate (pyrolysis stage) $(\frac{dm}{dT})_{max}$ / % K-1	−0.880 ± 0.02	−0.772 ± 0.03	−0.728 ± 0.03	−0.935 ± 0.06	−0.828 ± 0.03	−0.794 ± 0.01
Max. mass-loss rate (char combustion, air only) $(\frac{dm}{dT})_{max,char}$ / % K-1	-	-	-	−0.418 ± 0.02	−0.363 ± 0.02	−0.310 ± 0.02
Mass loss, pyrolysis stage (Stage II in air; Stage III in N_2) Δm_1 / %	67.3 ± 2.1	64.5 ± 2.7	65.5 ± 0.4	63.0 ± 3.9	64.0 ± 1.1	63.2 ± 1.2
Mass loss, char combustion (Stage III, air only) Δm_2 / %	-	-	-	25.1 ± 1.6	23.2 ± 2.3	13.3 ± 1.8

Parameter	N_2 atmosphere			Synthetic air atmosphere		
	β = 10 / °C min-1	β = 25 / °C min-1	β = 50 / °C min-1	β = 10 / °C min-1	β = 25 / °C min-1	β = 50 / °C min-1
Residual mass at *500 °C* / %	21.5 ± 1.9	24.6 ± 4.2	27.1 ± 0.4	4.6 ± 6.4	4.5 ± 3.5	15.4 ± 3.5*
Total mass loss Δm / %	78.0 ± 2.0	75.2 ± 4.2	72.7 ± 0.3	96.4 ± 6.0	95.5 ± 3.9	84.4 ± 3.4*

** Values are means ± 1 standard deviation. All mass values are expressed relative to the initial sample mass. For synthetic air at β = 50 °C min⁻¹, the values are based on two replicates because one replicate was not available; these data should therefore be interpreted with caution. $T_{max,char}$ and Δm_{char} apply only to the char-combustion stage under synthetic air. T_{end} for the pyrolysis stage was not resolved under synthetic air because of overlap with the subsequent char-combustion stage.*

Stage IV – Char consolidation and slow lignin decomposition (above 703 K). Above T_{max}, the mass-loss rate decreased progressively, reflecting the thermally stable, aromatic character of the lignin-derived carbonaceous char [5]. No distinct secondary DTG minimum was observed under nitrogen in this temperature range. The residual mass at 773 K (500 °C) was 21.5 ± 1.9% at β = 10 °C min-1, 24.6 ± 4.2% at β = 25 °C min-1, and 27.1 ± 0.4% at β = 50 °C min-1 (Table 1).

3.1.2 Effect of heating rate on characteristic temperatures and DTG intensity

The onset temperature T_{onset}increased from 536.5 ± 1.2 K (263.3 °C) at β = 10 °C min-1 to 543.9 ± 1.3 K (270.8 °C) at β = 50 °C min-1, a shift of 7.4 K across the investigated range (Table 1). T_{max} showed a more pronounced positive shift of 18.5 K (619.5 → 638.0 K from β = 10 to 50 °C min-1), reflecting the finite time required for the reaction to reach its maximum rate at each heating rate [15]. The endset temperature T_{end} shifted less substantially: from 686.2 ± 3.3 K (413.0 °C) to 692.1 ± 4.6 K (418.9 °C), a change of only 5.9 K. The peak DTG intensity $(\frac{dm}{dT})_{max}$ decreased monotonically with increasing β: from −0.880 ± 0.024 % K-1 at β = 10 °C min-1 to −0.728 ± 0.029 % K-1 at β = 50 °C min-1, reflecting the broadening of the decomposition event over a wider temperature interval at faster heating. All characteristic parameters are listed in Table 1.

3.2 DSC curves – nitrogen atmosphere

The DSC curves recorded under nitrogen are presented in Figure 2a (Netzsch sign convention: EXO = −1; negative signal = exothermic). The signal was predominantly negative throughout the temperature range 423–773 K, indicating a net exothermic character of the combined decomposition and char formation reactions. However, a distinct local maximum (least negative region, corresponding to an endothermic contribution) was resolved at T = 638 ± 3 K (365 °C) for β = 10 °C min-1, 654 ± 2 K (381 °C) for β = 25 °C min-1, and 665 ± 1 K (392 °C) for β = 50 °C min-1. This feature corresponds to the endothermic contribution of cellulose depolymerization, which momentarily reduces the net exothermic signal relative to the surrounding baseline. The temperature of this endothermic feature shifted by approximately 27 K between β = 10 and 50 °C min-1, consistent with the positive heating-rate dependence observed in the DTG data (Section 3.1.2). Above ~700 K (430 °C), the DSC signal became progressively more negative, reflecting exothermic char condensation and secondary polyaromatic reactions from lignin-derived intermediates. No distinct exothermic peak was resolved under nitrogen (N_2) within the investigated temperature range. The absolute DSC intensity scaled with heating rate: at β = 50 °C min-1, heat flow values were approximately 3–4 times more negative than at β = 10 °C min-1 across the entire range.

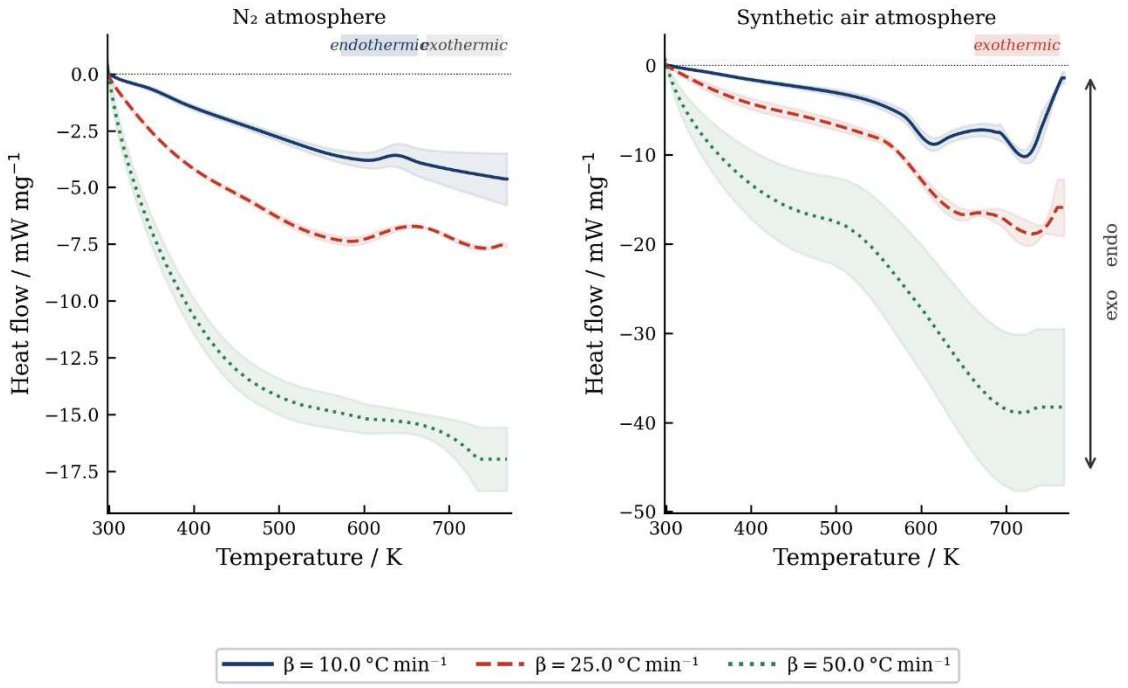

Figure 2. DSC curves of Norway spruce wood in (a) N_2 and (b) synthetic air atmospheres at β = 10, 25, and 50 °C min-1. Netzsch sign convention: negative signal = exothermic (EXO = −1). The endothermic contribution of cellulose depolymerization appears as a local maximum (least negative) in the 635–665 K region. The strongly exothermic peak in (b) above 700 K corresponds to char combustion (Stage III). Exo and endo directions are indicated by arrows. Shaded bands: ±1 standard deviation (SD).

3.3 TG and DTG curves – synthetic air atmosphere

3.3.1 Two-stage degradation profile

In synthetic air, the thermal degradation of spruce wood proceeded through two clearly resolved mass-loss stages, visible as two distinct minima in the DTG curves (Figure 3). The first stage (Stage II, oxidative pyrolysis) was centered at T_{max}, 1 = 594.0 ± 0.6 K (320.9 ± 0.6 °C) for β = 10 °C min-1, 613.2 ± 1.0 K (340.1 °C) for β = 25 °C min-1, and 612.5 ± 8.3 K (339.4 °C) for β = 50 °C min-1. The subsequent stage (Stage III, char combustion) appeared as a distinct DTG minimum at $T_{max}, char$ = 720.4 ± 2.7 K (447.3 °C) for β = 10 °C min-1 and 732.8 ± 16.6 K (459.6 °C) for β = 25 °C min-1. At β = 50 °C min-1 (n = 2), the Stage III peak showed high variability (T_{max},char = 692 ± 55 K); these values should be interpreted with caution. The total mass loss was 96.4% at β = 10 °C min-1 and 95.5% at β = 25 °C min-1 (Table 1).

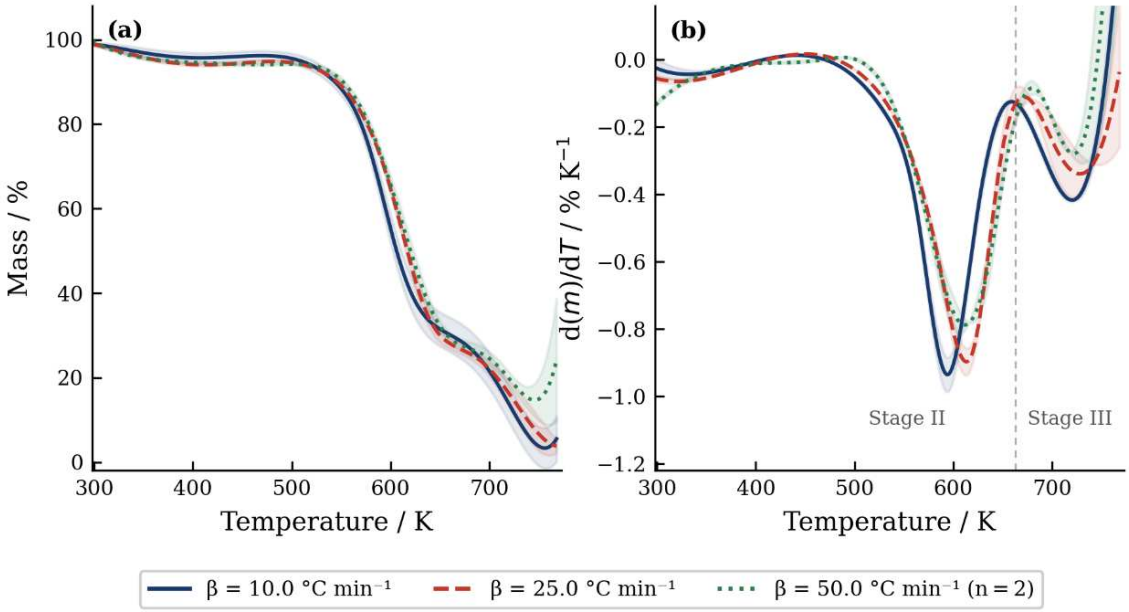

Figure 3. (a) TG curves and (b) DTG curves of Norway spruce wood recorded in synthetic air atmosphere at heating rates of 10, 25, and 50 °C min-1. Solid lines represent mean values; shaded bands indicate ±1 standard deviation. The vertical dashed line in (b) marks the boundary between Stage II (oxidative pyrolysis) and Stage III (char combustion). Data for β = 50 °C min-1 represent the mean of two replicates. Legend applies to both panels.

3.3.2 Stage II – oxidative pyrolysis (423–663 K)

The mass loss in Stage II was 63.0 ± 3.9% at β = 10 °C min-1, 64.0 ± 1.1% at β = 25 °C min-1, and 63.2 ± 1.2% at β = 50 °C min-1 (Table 1). T_{max}, 1 increased with heating rate from 594.0 K at β = 10 °C min-1 to 613.2 K at β = 25 °C min-1 (+19.2 K), analogous to the positive heating-rate dependence observed for T_{max}, 1 under nitrogen (Section 3.1.2). The peak DTG intensity of Stage II, $(\frac{dm}{dT})_{max}$, 1, was −0.935 ± 0.062 % K-1 at β = 10 °C min⁻¹ and decreased to −0.897 ± 0.049 % K-1 at β = 25 °C min⁻¹ and −0.799 ± 0.023 % K-1 at β = 50 °C min-1, reflecting the broadening of the mass-loss event at faster heating.

3.3.3 Stage III – char combustion (663–773 K)

A second distinct DTG minimum, corresponding to Stage III (char combustion), was recorded at $T_{max}, char$ = 720.4 ± 2.7 K (447.3 °C) at β = 10 °C min-1 and 732.8 ± 16.6 K (459.6 °C) at β = 25 °C min-1. The mass loss in this stage was 25.1 ± 1.6% at β = 10 °C min-1 and 23.2 ± 2.3% at β = 25 °C min-1. The corresponding peak DTG intensity, $(\frac{dm}{dT})_{max}, char$, was −0.418 ± 0.005 % K-1 at β = 10 °C min⁻¹ and −0.363 ± 0.049 % K-1 at β = 25 °C min-1. The residual mass at 773 K (500 °C) was 4.6% at β = 10 °C min-1 and 4.5% at β = 25 °C min-1, indicating near-complete combustion of the char formed during Stage II. At β = 50 °C min-1 (n = 2), the residual mass was substantially higher (15.4%) with large variability in $T_{max}, char$ (692 ± 55 K), attributable to the limited replication at this rate.

3.4 DSC curves – synthetic air atmosphere

The DSC profiles recorded under synthetic air are presented in Figure 2b (same sign convention as Figure 4a: EXO = −1). In the pyrolysis temperature range (423–663 K), the DSC signal was predominantly negative, with a local maximum (endothermic contribution) in the 594–613 K region corresponding to Stage II. Above 663 K, a strongly exothermic DSC peak emerged, corresponding to Stage III char combustion. The peak minimum was recorded at 723.1 ± 4.7 K (449.9 °C) for β = 10 °C min⁻¹ with a mean heat flow of −10.6 ± 0.7 mW mg-1, and at approximately 761 K (488 °C) for β = 25 °C min-1 (−19.3 mW mg-1). The absolute magnitude of the exothermic peak increased with heating rate, consistent with the proportionally higher power required to maintain the programmed ramp at faster rates.

3.5 Comparison of N_2 and air TG/DTG profiles

The characteristic temperatures, DTG peak intensities, and mass loss parameters for both atmospheres and all three heating rates are compiled in Table 1. The overlay of TG curves at identical heating rates (Figure 4) and the summary of T_{max} values as a function of β (Figure 5) highlight three systematic differences between the two atmospheres.

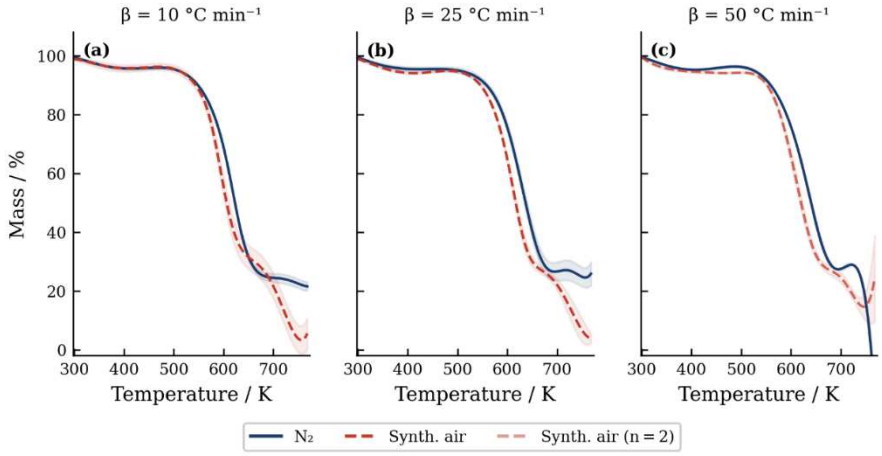

Figure 4. Comparison of TG curves recorded in N_2 (solid lines) and synthetic air (dashed lines) at (a) 10, (b) 25, and (c) 50 °C min-1. Shaded bands indicate ±1 standard deviation. Data for 50 °C min-1 in air represent the mean of two replicates.

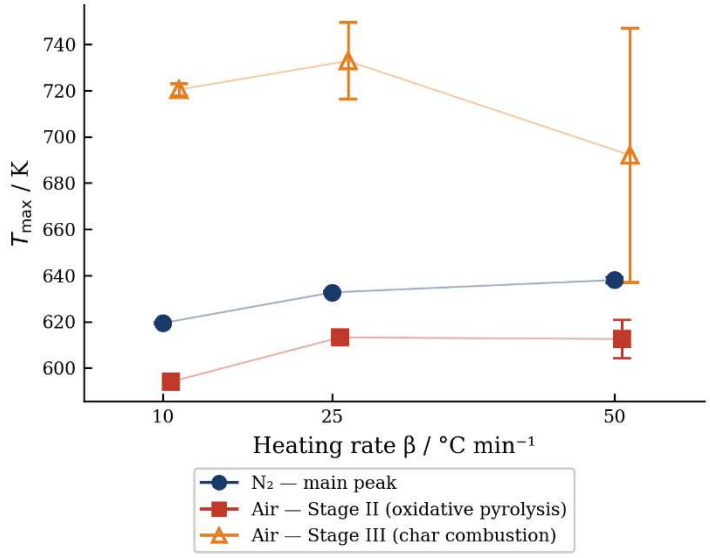

Figure 5. Temperature of maximum mass-loss rate T_{max} as a function of heating rate β, for N_2 (main peak), air Stage II (oxidative pyrolysis), and air Stage III (char combustion). Error bars represent ±1 standard deviation. Lines connect mean values as a guide to the eye.

First, the onset of mass loss was consistently lower under synthetic air: T_{onset} was on average 7.5 K lower in air than in nitrogen at the same β (255.8 vs. 263.3 °C at β = 10 °C min-1; Table 1), indicating an accelerating effect of oxygen on the initiation of thermal degradation.

Second, the primary DTG peak temperature was lower in air at each heating rate. At β = 10 °C min-1, T_{max}, 1 (air) = 594.0 K vs. T_{max} (N_2) = 619.5 K, a difference of 25.5 K. At β = 25 °C min-1, the difference was 19.5 K (613.2 vs. 632.7 K). This shift reflects the contribution of oxidative chain-scission pathways to the decomposition of the wood matrix under air. The DTG intensity of Stage II in air (−0.935 to −0.799 % K-1) was comparable to the Stage III peak under nitrogen (−0.880 to −0.728 % K-1), indicating a similar extent of primary devolatilization. The mass loss in the pyrolysis stage was similar under air (63.0–64.0%) and nitrogen (64.5–67.3%) within the

variability of the measurements, suggesting that the overall extent of primary devolatilization was not strongly affected by the presence of oxygen.

Third, the residual mass at 500 °C differed dramatically between the two atmospheres (Figure 6).

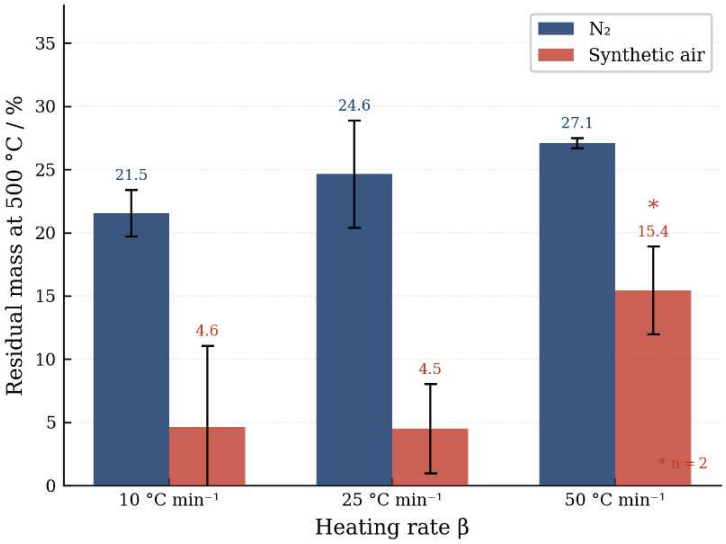

Figure 6. Residual mass at 500 °C (773 K) for N_2 and synthetic air atmospheres at each heating rate. Error bars: ±1 standard deviation. Values above bars indicate mean residual mass (%); asterisk (*) denotes result based on n = 2 replicates.

Under nitrogen, residual mass increased with heating rate: 21.5% (β = 10), 24.6% (β = 25), and 27.1% (β = 50 °C min-1). Under synthetic air, residual mass was below 5% at β = 10 and 25 °C min⁻¹ (4.6% and 4.5%, respectively), demonstrating near-complete combustion of the carbonaceous char during Stage III. The value at β = 50 °C min-1 (15.4%) is based on two replicates only and should be interpreted with caution.

Regarding the DSC profiles, the N_2 and air signals were qualitatively similar in the pyrolysis range (423–663 K), both showing a net exothermic baseline with a local endothermic maximum associated with cellulose depolymerization. Above 663 K, the two atmospheres diverged markedly: under air, a strongly exothermic peak emerged at 720–761 K (−10.6 to −19.3 mW mg-1), attributable to Stage III char combustion, while no equivalent exothermic feature was present under nitrogen. The magnitude of the air DSC peak was 3–5 times more negative than the maximum heat flow under nitrogen at comparable temperatures.

3.6 Kinetic analysis

3.6.1 Kissinger method

The Kissinger linearization of $\ln\left(\frac{\beta}{T_{max2}}\right)$ vs. $\frac{1}{T_{max}}$ (Figure 7) yielded an apparent activation energy of E_a = 262.1 kJ mol-1 (R^2 = 0.970) under nitrogen, based on T_{max} values of 619.5 K (β = 10 °C min⁻¹), 632.7 K (β = 25 °C min-1), and 638.0 K (β = 50 °C min⁻¹). Under synthetic air, the Stage II DTG peak yielded E_a = 190.1 kJ mol-1 (R^2 = 0.773), based on T_{max}, 1 of 594.0 K, 613.2 K, and 612.5 K at β = 10, 25, and 50 °C min-1, respectively. These values are used primarily as benchmark comparators; the iso-conversional results are considered the primary kinetic output [8–10].

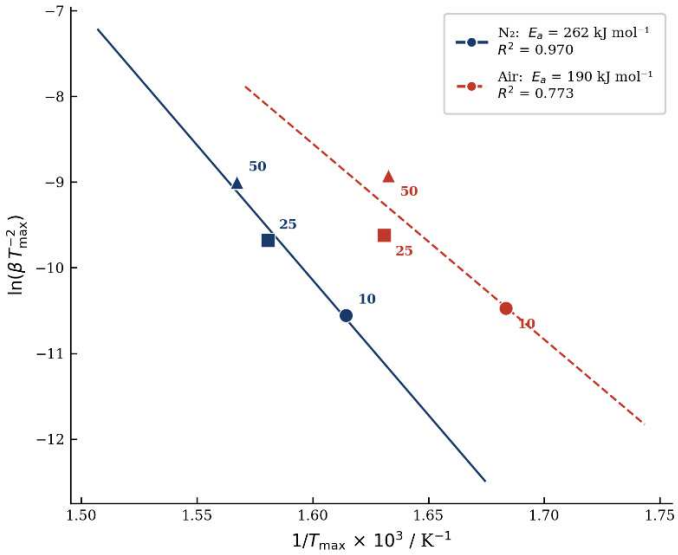

Figure 7. Kissinger plots for N_2 (filled circles, solid regression line) and synthetic air (filled squares, dashed regression line). Numbers beside symbols indicate the heating rate β in °C min-1. Apparent activation energies and coefficients of determination (R^2) are given in the legend.

3.6.2 OFW iso-conversional analysis

Under nitrogen, the OFW method yielded $E_a(\alpha)$ values ranging from 329.0 to 345.2 kJ mol-1 across $\alpha = 0.05$–0.90 (mean 340.5 ± 9.1 kJ mol-1; mean $R^2 = 0.82$). The $E_a(\alpha)$ profile was remarkably flat across $\alpha = 0.15$–0.85, with a variation of only 16 kJ mol-1. The KAS method returned systematically higher values of 336.5–352.8 kJ mol-1 (mean 347.9 ± 9.4 kJ mol-1; mean $R^2 = 0.81$), maintaining the same flat profile. All kinetic parameters are summarized in Table 2.

Under synthetic air, the OFW method yielded $E_a(\alpha)$ values of 302.1–378.4 kJ mol-1 across α = 0.05–0.60 (mean 325.9 ± 18.5 kJ mol-1; mean $R^2 = 0.61$). The KAS method returned 307.5–387.6 kJ mol-1 (mean 333.0 ± 19.4 kJ mol-1; mean $R^2 = 0.59$). The $E_a(\alpha)$ profiles for both atmospheres are shown in Figure 8; all kinetic parameters are compiled in Table 2.

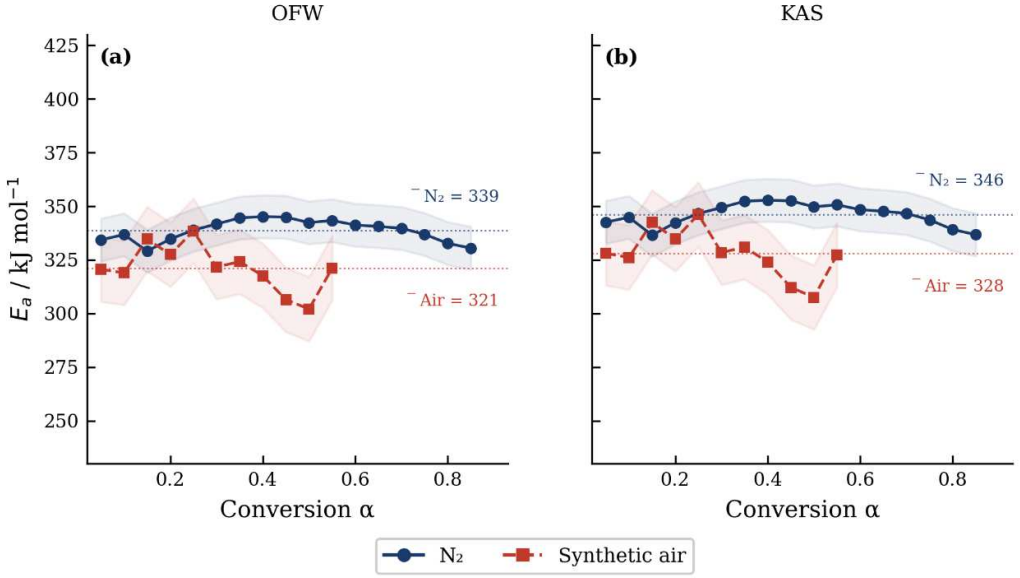

Figure 8. Activation energy E_a as a function of conversion α, determined by (a) the OFW method and (b) the KAS method, for N_2 (circles, solid lines) and synthetic air (squares, dashed lines). Shaded bands represent the uncertainty range of ±10 kJ mol-1 (N_2) and ±15 kJ mol-1 (air). Dotted horizontal lines indicate mean E_a values for each atmosphere; mean values are annotated

in each panel. The iso-conversional range for air is limited to α = 0.05–0.60 due to the two-mechanism character of the oxidative system (see text).

Table 2 Apparent activation energies E_a for thermal degradation of Norway spruce wood (Picea abies) under N_2 and synthetic air atmospheres, determined by the Kissinger, Ozawa–Flynn–Wall (OFW), and Kissinger–Akahira–Sunose (KAS) methods. T_{max} values used in the Kissinger analysis are listed below. OFW and KAS values represent means ± 1 SD over the conversion range α = 0.05–0.85.

Method	Atmosphere	E_α (kJ mol-1)	± SD (kJ mol-1)	R^2 (mean)	Conversion α
Kissinger	N_2	262.1	-	0.970	T_{max} only
	Synth. air	190.1	-	0.773	T_{max},1 only
OFW	N_2	338.7	4.9	0.813	0.05–0.85
	Synth. air	321.2	10.1	0.618	0.05–0.60*
KAS	N_2	346.0	5.1	0.804	0.05–0.85
	Synth. air	328.0	10.8	0.604	0.05–0.60*

T_{max} values used in the Kissinger analysis:

Atmosphere	β = 10 °C min-1	β = 25 °C min-1	β = 50 °C min-1	E_α (kJ mol-1)
N_2	619.4 K (346.3 °C)	632.7 K (359.5 °C)	638.0 K (364.9 °C)	262.1
Synth. air (Stage II)	594.0 K (320.9 °C)	613.2 K (340.0 °C)	612.5 K (339.3 °C)	190.1

** Conversion range limited to α = 0.05–0.60 for air due to mechanistic complexity of the two-stage oxidative system and limited replication at β = 50 °C min-1 (n = 2). R^2 values for air are lower than for N_2, reflecting the two-mechanism character of oxidative degradation. OFW: Ozawa–Flynn–Wall method; KAS: Kissinger–Akahira–Sunose method.*

4 Discussion

4.1 Multi-component degradation mechanism under nitrogen

The four-stage degradation profile identified under nitrogen is fully consistent with the established parallel-reaction framework for wood pyrolysis [5–7]. In Norway spruce, galactoglucomannan (approximately 20 wt% of dry wood) begins deacetylation and random-chain scission below 493 K, generating acetic acid, mannose, and furfural derivatives as primary products [5]. The relatively poor resolution of this shoulder in the DTG curves at higher heating rates is characteristic of softwoods, whose hemicellulose fraction decomposes more gradually and at overlapping temperatures with the onset of cellulose decomposition, compared with the sharper hemicellulose step observed in hardwoods [7].

The dominant Stage III (cellulose depolymerization) produced a sharp, symmetric DTG minimum with excellent reproducibility across replicates (SD of $T_{max} \leq 1.3$ K at all heating rates), confirming the cooperative and mechanistically well-defined character of cellulose pyrolysis. The endothermic DSC signal resolved as a local maximum at ~638–665 K is consistent with the heat of depolymerization of crystalline cellulose ($\Delta H \approx +50$ to +80 J g^{-1} reported in the literature), which absorbs energy as glycosidic bonds are cleaved and the crystalline order is disrupted [5]. Above ~700 K, the net DSC signal became increasingly exothermic, reflecting lignin condensation and polyaromatic graphitization reactions, which are known to be exothermic ($\Delta H \approx -20$ to -60 J g^{-1}) [5].

The near-constant $E_\alpha(\alpha)$ profile under nitrogen (OFW range: 329–345 kJ mol-1 across α = 0.15–0.85) indicates that the main conversion interval is governed by a dominant apparent degradation process, which can be attributed primarily to cellulose depolymerization, while hemicellulose and lignin reactions contribute less strongly to the iso-conversional signal in this range. This finding is consistent with the much lower DTG intensity of Stages II and IV relative to Stage III and validates the use of a pseudo-single-component kinetic description for the main degradation event in Norway spruce under nitrogen.

4.2 Non-equilibrium effects of heating rate

The systematic positive shift of T_{max} with β (18.6 K in N_2, 19.2 K in air between 10 and 25 °C min-1) is a classical kinetic consequence of the finite time available for reaction at each temperature during a linear temperature ramp

[15]. The increasing residual mass with β under nitrogen (21.5 → 27.1%) is a direct manifestation of non-equilibrium pyrolysis: at higher heating rates, the temperature traverses the primary decomposition window faster than the secondary reactions (volatilization and char gasification) can reach completion, resulting in a higher fraction of carbon retained in the solid phase [18]. This effect is of direct relevance to fast-pyrolysis bio-oil production, where the elevated heating rates required for maximum liquid yield can paradoxically increase char formation if particle residence times are not optimized.

The conditions imposed at β = 50 °C min-1 constitute a thermodynamically non-equilibrium regime in a physically precise sense. Mehrabian et al. [19] established that 50 K min-1 marks the boundary above which the instantaneous pyrolysis rate of biomass particles in combustion and gasification systems consistently exceeds the capacity of conventional TGA kinetics to describe it. The observation in the present study that char yield increased monotonically from 21.5% at β = 10 °C min-1 to 27.1% at β = 50 °C min-1 under nitrogen is a direct kinetic manifestation of this non-equilibrium character: the system does not have sufficient residence time at each temperature to maximize volatile release, diverting a greater fraction of carbon into the solid char phase [3, 20]. This behavior has been documented across a broad range of lignocellulosic substrates and represents a fundamental departure from the equilibrium product distribution predicted by slow-heating kinetic models [3]. The increase in residual mass under nitrogen at β = 50 °C min-1 suggests that secondary char-forming pathways become more important when the material is heated more rapidly through the main decomposition interval. This interpretation is consistent with the general understanding that rapid heating can alter the balance between volatilisation and solid-phase carbon retention. However, because direct molecular analysis of volatile products was not performed, the proposed shift in product distribution should be treated as an interpretation based on thermal behavior rather than as direct chemical evidence.

Despite the non-equilibrium conditions at β = 50 °C min-1, the iso-conversional $E_a(\alpha)$ profile under nitrogen remained flat and consistent with lower heating rate results (OFW: 329–345 kJ mol-1). This indicates that the dominant reaction mechanism does not change qualitatively within the 10–50 °C min-1 range, and that kinetic parameters determined from conventional lower-rate experiments remain applicable for predicting degradation behavior at moderately elevated heating rates. The decreasing DTG peak intensity with β (expressed per unit temperature) is a purely mathematical consequence of event broadening and does not imply a change in the total conversion extent, which remained stable at 64–68% across all heating rates.

4.3 Atmosphere effects: pyrolysis vs. oxidative degradation

The lower T_{onset} and T_{max}, 1 under air compared with nitrogen (by 7.5 K and 25 K, respectively, at β = 10 °C min-1) demonstrate that molecular oxygen provides an alternative, lower-energy pathway for the initiation and propagation of chain scission in both hemicellulose and cellulose. The presence of oxygen may facilitate oxidative degradation pathways and accelerate the onset of mass loss, thereby lowering the observable characteristic temperatures compared with inert conditions [16]. The comparable mass loss in Stage II under air (63.0%) and Stage III under N_2 (67.3%) at β = 10 °C min-1 confirms that the total devolatilization extent is not significantly altered by atmosphere: it is determined primarily by the chemical composition of the wood (cellulose, hemicellulose, and volatile lignin fractions), not by the degradation pathway.

The strongly exothermic DSC peak at 723–761 K in air (−10.6 to −19.3 mW mg-1), absent entirely under nitrogen, unambiguously identifies Stage III as heterogeneous char combustion. The magnitude of this exothermic signal (3–5 times the peak heat flow under N_2) and the near-complete mass loss at 773 K (residue < 5%) are consistent with the complete oxidation of a char structure, which is known to be reactive toward oxygen at temperatures above 650 K [17]. From a fire safety perspective, this exothermic Stage III event significantly amplifies the thermal hazard of burning spruce [26]: the heat release from char combustion sustains and accelerates the temperature rise in the wood surface layer, contributing to flame spread and glowing combustion persistence after the volatile flame extinguishes.

The lower onset temperature in air also has direct implications for the piloted ignition threshold of Norway spruce. The temperature at which sustained mass loss and flammable volatile generation begin is reduced by approximately 7–8 K in an oxidative atmosphere compared with pyrolytic conditions, consistent with field observations that wood

surfaces in contact with a heated airflow ignite more readily than those in radiant heating without convective oxidation [16].

4.4 Comparison and validity of kinetic methods

The three methods applied yielded activation energies that are mutually consistent in their relative ordering (Kissinger < OFW < KAS) and qualitatively agree in the atmosphere comparison trend (N_2 > air). The OFW–KAS offset of ≈7 kJ mol-1 in both atmospheres is attributable to the less accurate Doyle approximation of the temperature integral used in OFW, which systematically underestimates E_a relative to the more precise Coats–Redfern approximation of KAS [8, 10]. For nitrogen, the iso-conversional regressions showed acceptable linearity over the selected conversion range, supporting the use of OFW and KAS for the main degradation interval. For synthetic air, the lower R^2 values indicate that the apparent activation energies should be interpreted more cautiously.

The substantially lower Kissinger E_a (262 kJ mol-1 in N_2) relative to OFW/KAS (~341–348 kJ mol-1) reflects both the theoretical limitations of the Kissinger method and the partial contribution of hemicellulose and low-temperature lignin reactions to the DTG peak position. The Kissinger method samples only the peak region, where Stage II (hemicellulose) and Stage III (cellulose) overlap and the effective E_a is a mixture of both component contributions. By contrast, the iso-conversional methods at α = 0.40–0.60 sample primarily the cellulose-dominated central conversion window, yielding a purer measure of the cellulose depolymerization kinetics. The ICTAC Kinetics Committee explicitly recommends iso-conversional methods over peak-based methods for multi-component systems [8 – 10].

The mean KAS E_a = 347.9 kJ mol-1 under nitrogen is higher than the component-resolved activation energy for cellulose of 236 kJ mol-1 reported by Grønli et al. [7] for a three-parallel-reactions model. This difference is expected: the iso-conversional method applied to the whole wood sample captures the combined, apparent E_a of all simultaneously decomposing components, whereas the three-component model isolates the individual contribution of cellulose after deconvolving the DTG curve. The higher apparent value obtained here is consistent with published iso-conversional results for whole wood, which typically fall in the range 160–370 kJ mol-1 depending on species, temperature range, and analytical procedure [8, 16, 27].

For the air atmosphere, the lower R^2 values of the iso-conversional regressions (mean 0.59–0.61 vs. 0.81–0.82 for N_2) and the higher variability of $E_a(\alpha)$ are attributable to two compounding factors: (i) the incomplete replication at β = 50 °C min-1 (n = 2), which reduces the precision of the average Tα at this rate; and (ii) the mechanistic complexity of the oxidative system, in which the measured conversion at any temperature is the aggregate result of both pyrolytic and oxidative decomposition, two processes with different activation energies. Completion of the triplicate at β = 50 °C min-1 and extension of the analysis to include a Friedman differential iso-conversional method would be recommended to improve the reliability of the air kinetic parameters.

4.5 Implications for fire behavior and thermochemical conversion

The combined STA dataset provides a self-consistent experimental basis for kinetic parameterization of Norway spruce degradation in both pyrolytic and oxidative regimes. The characteristic temperatures (T_{onset}, T_{max}, T_{end}) and iso-conversional $E_a(\alpha)$ profiles are directly applicable as input parameters for pyrolysis submodels in computational fire simulation tools such as FDS (Fire Dynamics Simulator) [28], where the temperature and rate of volatile generation govern ignition and flame spread predictions.

The upper heating rate of 50 °C min-1 is of particular relevance in this context: surface heating rates in this range have been documented during the growth phase of compartment fires in timber structures [20], indicating that the kinetic parameters reported here span the transition from conventional analytical conditions to the non-equilibrium regime encountered in real fire scenarios. Extrapolation of the present iso-conversional $E_a(\alpha)$ data beyond 50 °C min-1 should be approached with caution and would require complementary high-rate experiments using, for example, a wire-mesh reactor or a drop-tube furnace.

The identification of the two-stage profile under air, with its strongly exothermic Stage III at 720–760 K, is particularly relevant for modeling glowing combustion and afterburn behavior in structural timber fires [26, 28].

For bioenergy applications, the results confirm that Norway spruce pyrolysis at moderate heating rates (10–25 °C min-1) produces a substantial char residue (21–25%) under nitrogen, which is relevant for biochar yield estimation. The increasing char residue at β = 50 °C min-1 (27.1%) aligns with reports of higher char yields in fast pyrolysis reactors when particle heating rates exceed ~100 °C min-1, though extrapolation beyond the investigated rate range requires caution. Direct chemical identification of volatile products was not included in the present study. Therefore, the implications for product distribution and reaction pathways should be regarded as thermal-kinetic interpretations rather than molecularly resolved conclusions.

4.6 Limitations and need for complementary chemical analysis

The present study provides a robust thermal and kinetic characterization of Norway spruce degradation under inert and oxidative atmospheres; however, it does not include direct molecular identification of volatile degradation products. Consequently, the assignment of individual degradation stages to hemicellulose, cellulose and lignin transformations is based on the combined TG/DTG/DSC response and comparison with established literature on lignocellulosic decomposition. This approach is sufficient for kinetic interpretation, but it does not allow the temperature-dependent distribution of furans, anhydro sugars, carbonyl compounds or phenolic products to be quantified.

Future work should therefore combine the STA-derived characteristic temperatures with pyrolysis–GC–MS or evolved gas analysis in order to verify the molecular composition of volatile products released at the onset, maximum-rate and endset regions of the main degradation stage. Such complementary analysis would strengthen the mechanistic interpretation of the non-equilibrium product shifts suggested by the increasing char yield at higher heating rates, particularly under nitrogen.

5. Conclusions

The non-isothermal thermal degradation of Norway spruce wood (Picea abies) was characterized by simultaneous TG/DSC analysis at heating rates of 10, 25 and 50 °C min-1 under nitrogen and synthetic air atmospheres, combined with model-free iso-conversional kinetic analysis. Under nitrogen, four thermally distinct degradation regions were identified: moisture release, hemicellulose decomposition, a dominant cellulose-related mass-loss stage and high-temperature char consolidation. The main DTG peak shifted from 619.5 to 638.0 K as the heating rate increased from 10 to 50 °C min-1, while the residual mass at 500 °C increased from 21.5 to 27.1%. These results indicate enhanced char retention under moderately elevated heating-rate conditions.

Under synthetic air, two principal mass-loss stages were observed, corresponding to oxidative pyrolysis of the wood matrix and subsequent char combustion. The main degradation peak occurred at lower temperature than under nitrogen, and the char-combustion stage was accompanied by a strong exothermic DSC response above 700 K. Residual mass at 500 °C was below 5% at 10 and 25 °C min-1, demonstrating near-complete oxidation of the char residue under these conditions. The values obtained at 50 °C min-1 under synthetic air should be interpreted with caution because they are based on two replicates and show higher variability.

The Kissinger method yielded apparent activation energies of 262.1 kJ mol-1 under nitrogen and 190.1 kJ mol-1 under synthetic air. The OFW and KAS iso-conversional methods showed a nearly constant activation-energy profile under nitrogen, indicating a dominant apparent degradation process in the main conversion interval. Under synthetic air, lower R^2 values and greater variability reflected the overlapping contribution of pyrolytic and oxidative reactions. The dataset provides useful thermal and kinetic parameters for interpreting spruce wood degradation under inert and oxidative atmospheres and for supporting further modelling of wood pyrolysis, char formation and oxidative degradation.

The present study was limited to thermal and kinetic analysis. Future work may combine the STA-derived characteristic temperatures with pyrolysis–GC–MS or evolved gas analysis to verify the molecular composition of degradation products associated with the identified thermal stages..

References

[1] Vassilev SV, Baxter D, Andersen LK, Vassileva CG. An overview of the chemical composition of biomass. Fuel. 2010;89(5):913–933. https://doi.org/10.1016/j.fuel.2009.10.022

[2] Mohan D, Pittman CU Jr, Steele PH. Pyrolysis of wood/biomass for bio-oil: a critical review. Energy Fuels. 2006;20(3):848–889. https://doi.org/10.1021/ef0502397

[3] Di Blasi C. Modeling chemical and physical processes of wood and biomass pyrolysis. Prog Energy Combust Sci. 2008;34(1):47–90. https://doi.org/10.1016/j.pecs.2006.12.001

[4] Tapasvi D, Khalil R, Várhegyi G, Tran KQ, Grønli M, Skreiberg Ø. Thermal decomposition kinetics of woods with an emphasis on torrefaction. Energy Fuels. 2013;27(10):6134–6145. https://doi.org/10.1021/ef4016075

[5] Yang H, Yan R, Chen H, Lee DH, Zheng C. Characteristics of hemicellulose, cellulose and lignin pyrolysis. Fuel. 2007;86(12–13):1781–1788. https://doi.org/10.1016/j.fuel.2006.12.013

[6] Wang S, Dai G, Yang H, Luo Z. Lignocellulosic biomass pyrolysis mechanism: a state-of-the-art review. Prog Energy Combust Sci. 2017;62:33–86. https://doi.org/10.1016/j.pecs.2017.05.004

[7] Grønli MG, Várhegyi G, Di Blasi C. Thermogravimetric analysis and devolatilization kinetics of wood. Ind Eng Chem Res. 2002;41(17):4201–4208. https://doi.org/10.1021/ie0201157

[8] Vyazovkin S, Burnham AK, Criado JM, Pérez-Maqueda LA, Popescu C, Sbirrazzuoli N. ICTAC Kinetics Committee recommendations for performing kinetic computations on thermal analysis data. Thermochim Acta. 2011;520(1–2):1–19. https://doi.org/10.1016/j.tca.2011.03.034

[9] Vyazovkin S, Burnham AK, Favergeon L, Koga N, Moukhina E, Pérez-Maqueda LA, Sbirrazzuoli N. ICTAC Kinetics Committee recommendations for analysis of multi-step kinetics. Thermochim Acta. 2020;689:178597. https://doi.org/10.1016/j.tca.2020.178597

[10] Koga N, Vyazovkin S, Burnham AK, Favergeon L, Muravyev NV, Pérez-Maqueda LA, Saggese C, Sánchez-Jiménez PE. ICTAC Kinetics Committee recommendations for analysis of thermal decomposition kinetics. Thermochim Acta. 2023;719:179384. https://doi.org/10.1016/j.tca.2022.179384

[11] White JE, Catallo WJ, Legendre BL. Biomass pyrolysis kinetics: a comparative critical review with relevant agricultural residue case studies. J Anal Appl Pyrolysis. 2011;91(1):1–33. https://doi.org/10.1016/j.jaap.2011.01.004

[12] Ozawa T. A new method of analyzing thermogravimetric data. Bull Chem Soc Jpn. 1965;38(11):1881–1886. https://doi.org/10.1246/bcsj.38.1881

[13] Flynn JH, Wall LA. A quick, direct method for the determination of activation energy from thermogravimetric data. J Polym Sci B Polym Lett. 1966;4(5):323–328. https://doi.org/10.1002/pol.1966.110040504

[14] Akahira T, Sunose T. Method of determining activation deterioration constant of electrical insulating materials. Res Rep Chiba Inst Technol (Sci Technol). 1971;16:22–31. [no DOI; Scopus indexed]

[15] Kissinger HE. Reaction kinetics in differential thermal analysis. Anal Chem. 1957;29(11):1702–1706. https://doi.org/10.1021/ac60131a045

[16] Orfão JJM, Antunes FJA, Figueiredo JL. Pyrolysis kinetics of lignocellulosic materials—three independent reactions model. Fuel. 1999;78(3):349–358. https://doi.org/10.1016/S0016-2361(98)00156-2

[17] Manyà JJ, Velo E, Puigjaner L. Kinetics of biomass pyrolysis: a reformulated three-parallel-reactions model. Ind Eng Chem Res. 2003;42(3):434–441. https://doi.org/10.1021/ie020218p

[18] Bridgwater AV. Review of fast pyrolysis of biomass and product upgrading. Biomass Bioenergy. 2012;38:68–94. https://doi.org/10.1016/j.biombioe.2011.01.048

[19] Mehrabian R, Scharler R, Obernberger I. Effects of pyrolysis conditions on the heating rate in biomass particles and applicability of TGA kinetic parameters in particle thermal conversion modelling. Fuel. 2012;93:567–575. https://doi.org/10.1016/j.fuel.2011.09.062

[20] Bryden KM, Ragland KW, Rutland CJ. Modeling thermally thick pyrolysis of wood. Biomass Bioenergy. 2002;22(1):41–53. https://doi.org/10.1016/S0961-9534(01)00060-5

[21] Branca C, Giudicianni P, Di Blasi C. GC/MS characterization of liquids generated from low-temperature pyrolysis of wood. Ind Eng Chem Res. 2003;42(14):3190–3202. https://doi.org/10.1021/ie030066d

[22] Shen DK, Gu S. The mechanism for thermal decomposition of cellulose and its main products. Bioresour Technol. 2009;100(24):6496–6504. https://doi.org/10.1016/j.biortech.2009.06.095

[23] Asmadi M, Kawamoto H, Saka S. Thermal reactivities of catechols/pyrogallols and cresols/xylenols as lignin pyrolysis intermediates. J Anal Appl Pyrolysis. 2011;92(1):76–87. https://doi.org/10.1016/j.jaap.2011.04.012

[24] Fischer O, Lemaire R, Bensakhria A. Thermogravimetric analysis and kinetic modeling of the pyrolysis of different biomass types by means of model-fitting, model-free and network modeling approaches. J Therm Anal Calorim. 2024;149:5499–5522. https://doi.org/10.1007/s10973-023-12868-w

[25] Bradbury AGW, Sakai Y, Shafizadeh F. A kinetic model for pyrolysis of cellulose. J Appl Polym Sci. 1979;23(11):3271–3280. https://doi.org/10.1002/app.1979.070231112

[26] Zachar M, Čabalová I, Kačíková D, Zacharová L. The effect of heat flux to the fire-technical and chemical properties of spruce wood (Picea abies L.). Materials. 2021;14(17):4989. https://doi.org/10.3390/ma14174989

[27] Emiola-Sadiq T, Zhang L, Dalai AK. Thermal and kinetic studies on biomass degradation via thermogravimetric analysis: a combination of model-fitting and model-free approach. ACS Omega. 2021;6(26):16660–16671. https://doi.org/10.1021/acsomega.1c02937

[28] Rinta-Paavola A, Hostikka S. A model for the pyrolysis of two Nordic structural timbers. Fire Mater. 2022;46(1):97–113. https://doi.org/10.1002/fam.2947

[29] Vassilev SV, Baxter D, Andersen LK, Vassileva CG. An overview of the chemical composition of biomass. Fuel. 2010;89(5):913–933. https://doi.org/10.1016/j.fuel.2009.10.022